Optical Materials 79 (2018) 115–119

Contents lists available at ScienceDirect

Optical Materials

journal homepage: www.elsevier.com/locate/optmat

Sol-gel synthesis of Cu-doped *p*-CdS nanoparticles and their analysis as *p*-CdS/*n*-ZnO thin film photodiode

Sandeep Arya[a,*], Asha Sharma[a], Bikram Singh[a], Mohammad Riyas[a], Pankaj Bandhoria[b], Mohammad Aatif[c], Vinay Gupta[c]

[a] Department of Physics, University of Jammu, Jammu, 180006, J&K, India
[b] Department of Physics, Government Gandhi Memorial Science College, Jammu, 180001, J&K, India
[c] Advanced Materials and Devices Division, CSIR-National Physical Laboratory, New Delhi, 110012, India

ARTICLE INFO

Keywords:
Cu-doped CdS nanoparticles
p-CdS/*n*-ZnO heterojunction
Sol-gel method
Photo-response

ABSTRACT

Copper (Cu) doped *p*-CdS nanoparticles have been synthesized via sol-gel method. The as-synthesized nanoparticles were successfully characterized and implemented for fabrication of Glass/ITO/*n*-ZnO/*p*-CdS/Al thin film photodiode. The fabricated device is tested for small (−1 V to +1 V) bias voltage. Results verified that the junction leakage current within the dark is very small. During reverse bias condition, the maximum amount of photocurrent is obtained under illumination of 100 μW/cm^2. Electrical characterizations confirmed that the external quantum efficiency (EQE), gain and responsivity of *n*-ZnO/*p*-CdS photodiode show improved photo response than conventional *p*-type materials for such a small bias voltage. It is therefore revealed that the Cu-doped CdS nanoparticles is an efficient *p*-type material for fabrication of thin film photo-devices.

1. Introduction

Semiconductor materials exhibit potential characteristics to enhance the quality of light energy harvesting devices. Attempts are being made to devise new inorganic structures that can work efficiently toward light energy conversion [1]. A few economical nano-devices fabricated at standard temperature and pressures (STP) with excellent efficiencies have meanwhile been reported [2]. However, comprehensive research is required in the field of electronic materials to develop reliable photovoltaic (PV) modules over a large area at a low-cost [3]. The efficiency of PV devices depends on the carrier mobility of donors and acceptors. Researchers are investigating several inorganic materials for high electron mobility. Cadmium Sulfide (CdS) is a material of intense scientific research due to the wide variety of potential applications ranging from photovoltaic to luminescent devices [4–6]. It is an important *n*-type semiconductor that exhibits conductivity induced by sulphur vacancies due to excess cadmium atoms. This semiconductor is attractive due to the relatively large direct band gap of 2.42 eV at 300 K that absorbs light in the visible wavelength range with an absorption peak at 515 nm [7]. CdS nanoparticles show quantum size effect and is directly related to the absorption wavelength. CdS possesses an outstanding visible light detecting property among the other semiconductors and play an important role in determining the electronic properties [8]. It can crystallize in different structures upon size reduction, depending upon the reaction conditions [9]. Due to ease of availability, simple preparation and excellent optical properties, CdS nano-materials have been investigated for more than one pragmatic field including photochemical catalysis, gas sensor, detectors for laser and infrared, solar cells, non-linear optical materials, luminescence devices, optoelectronic devices and so on [10]. The doping of transition metal ions such as Mn, Cu, Co, opens up the probabilities of forming a new class of material with enhanced properties [11].

This work presents the synthesis method of *p*-CdS nanoparticles by doping the copper (Cu) into its chemical composition. The as-synthesized CdS nanoparticles were employed for the fabrication of photodiode and their analysis was carried out using thin films, particularly, *n*-ZnO and *p*-CdS thin film layers. The Hall Effect principle was used for the carrier mobility measurement and thus *p*-type conductivity of the as-synthesized CdS nanoparticles is verified. A complete arrangement of photodiode consists of different layers of chalcogenide materials which were deposited by spin coater followed by depositing the aluminium (Al) electrode via vacuum thermal evaporation deposition system.

2. Experiment

The whole experiment is divided into two sections- (A) Synthesis of Cu-doped CdS nanoparticles, and (B) device formation using as-synthesized nanoparticles.

* Corresponding author.
E-mail address: snp09arya@gmail.com (S. Arya).

https://doi.org/10.1016/j.optmat.2018.03.035
Received 9 January 2018; Received in revised form 10 February 2018; Accepted 20 March 2018
Available online 12 April 2018
0925-3467/

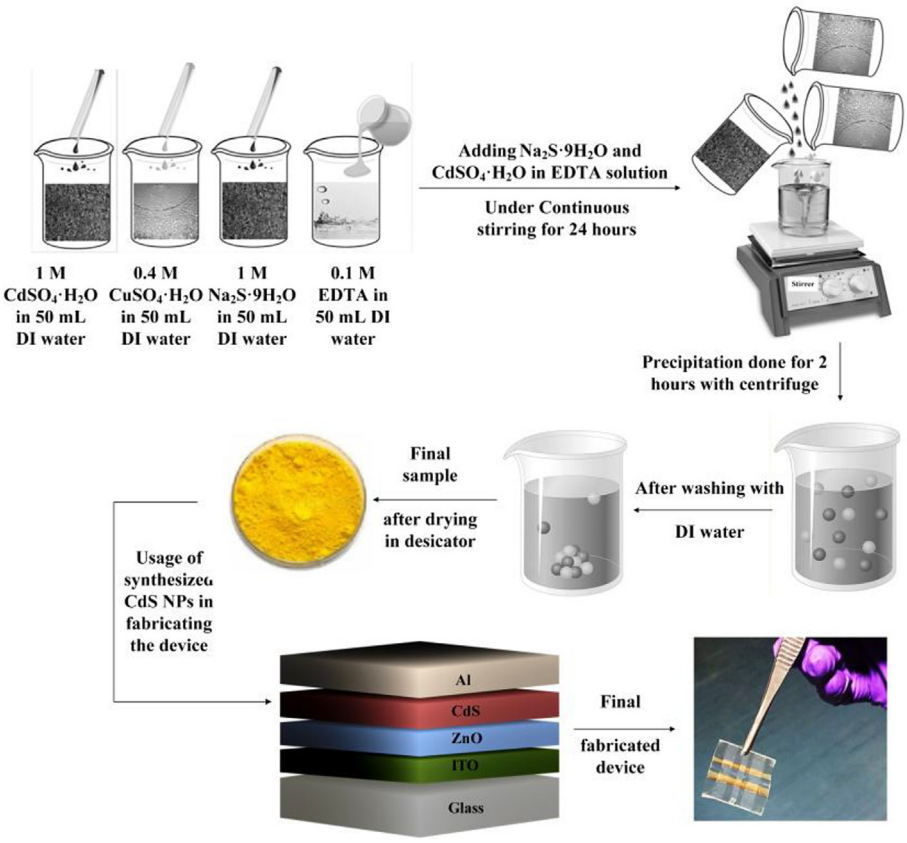

Fig. 1. Schematic diagram showing experimental steps performed for synthesizing Cu-doped CdS nanoparticles to fabricate the photodiode device on ITO coated glass substrate.

2.1. Synthesis of Cu-doped CdS nanoparticles

Synthesis of Cu-doped CdS nanoparticles is done by sol-gel method. The schematic for the formation of the proposed nanoparticles is shown in Fig. 1. Cu-doped CdS nanoparticles were prepared at 300 K by dropping simultaneously 50 ml aqueous solution of cadmium sulphate (1 M) along with the 50 ml aqueous solution of copper sulphate (0.4 M), and 50 ml of the molar solution of sodium sulphide (1 M) into 200 ml of distilled water containing 50 ml of 0.1 M solution of EDTA, which was vigorously stirred using a magnetic stirrer. The high insolubility of CdS formed out of the chemical reaction caused the formation of several new nuclei while restraining the growth of already existing ones, thus limiting the particle size. The precipitates were separated from the reaction mixture using a centrifuge and were dried in the desiccator at room temperature. After sufficient drying, the precipitate was crushed to a fine powder with the help of mortar and pestle. Thus, Cu-doped CdS nanoparticles were synthesized and hence characterized for further studies. Finally, the as-synthesized nanoparticles were further employed to fabricate a thin film layered photo device.

2.2. Device formation

For device fabrication, ITO coated glasses (luminescence technology corp. Taiwan, with a sheet resistance of 15 ?sq^{-1} and transmittance > 85%) were first patterned using laser writer System according to the proposed designed in MEMS designing software (Clewin) and then cleaned with soap, DI water, acetone and isopropanol under ultrasonication for 2 h followed by UV ozone treatment for 15 min. The as-prepared *n*-ZnO nanoparticles reported in Ref. [12] was dissolved in $C_3H_8O_2$ to form a colloidal solution and we spin-coated on ITO coated glass substrate at 4500 rpm, an acceleration of 500, for 1 min. The ZnO coated thin film was then annealed at 200 °C for 1 h in air. The thickness of films was ~30 nm, determined by a Profilometer. Further, 0.5 mg of as-synthesized *p*-CdS nanoparticles was dissolved in 2 ml solution of C_4H_8O to form a colloidal solution after sonication for 30 min. The solution was spin-coated on ZnO film in a N_2 filled modular glove box workstation (MB 200 B) at 1000 rpm for 1 min. The approximate thickness of the film was 50 nm. The coated films were annealed at 100 °C for 10 min to evaporate residual solvent and to achieve the optimum result. Finally, the device was coated using the shadow mask by thermal evaporation of 100 nm Al electrodes as anode. Thus, a thin film based glass/ITO/*n*-ZnO/*p*-CdS/Al heterojunction photo-device is fabricated. Further, the fabricated photo device with pixel area 0.045 cm^2 is tested to obtain the electrical characteristics.

3. Results and discussions

The as-synthesized nanoparticles were characterized through XRD, EDS, SEM, UV-Vis and PL spectrometry. Further, the fabricated photo-device by involving as-synthesized nanoparticles was studied for their I-V characteristics.

3.1. XRD characterization

The crystallinity of the Cu-doped CdS nanoparticles were examined by XRD analysis and the results are presented as Fig. 2(a). The prominent peaks at 2θ = 24.7°, 26.4°, 27.5°, 36.5°, 43.7°, 47.5°, and 51.6° corresponding to the reflections at (100), (002), (101), (102), (110), (103), and (112) planes were observed respectively. All the observed diffraction reflections are in good agreement with standard hexagonal phase of CdS (JCPDS 41–1049). Almost every observed XRD reflections are highly intense which confirmed that the as-synthesized nanoparticles are well crystalline. The doping of Cu in CdS nanoparticles does not create any major change in the CdS matrix. The particle size was also calculated using the Scherrer's formula [13], i.e.

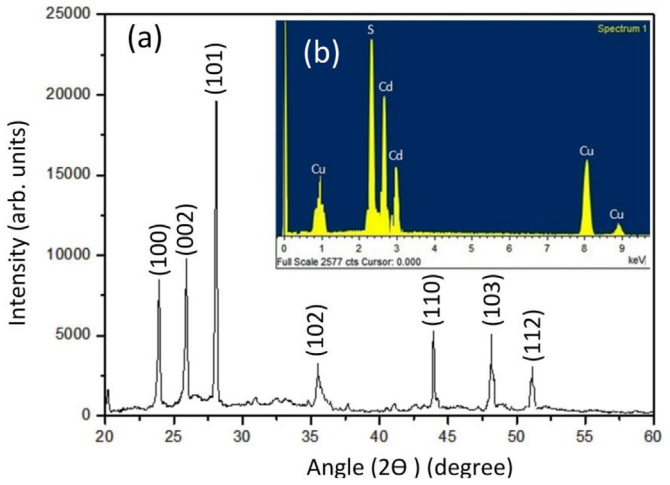

Fig. 2. (A) XRD pattern, and (b) EDS compositional intensity, of as-synthesized Cu-doped CdS nanoparticles.

$$D = \frac{k\lambda}{\beta \cos\theta} \tag{1}$$

where D is the average particle size perpendicular to the reflecting planes, λ is the X-ray wavelength, k is constant and is equal to 0.9, β is the full width at half maximum (FWHM), and θ is the diffraction angle. The average particle size was found to be 66.31 nm respectively.

3.2. EDS characterization

The elemental compositions of the as-synthesized Cu-doped CdS nanoparticles is observed by EDS and results are shown in Fig. 2(b). This is an automated generated graph by built-in software and shows the highest counts of Sulphur. From the EDS spectrum shown in Fig. 2(b), it can be observed that the dominated peaks belong to Cadmium, Copper and Sulphur which reveal that the synthesized products is made of these three elements. Percentage (%) composition of the elements present in sample of Cu-doped CdS nanoparticles are shown in Table 1. No other dominated peak is observed in the spectrum which clearly revealed that the synthesized material is in pure form.

3.3. SEM characterization

Fig. 3 shows the surface morphology of the *p*-CdS nanoparticles that were analyzed by using scanning electron microscopy (SEM). Fig. 3(a) shows the SEM micrograph (top view) of as-synthesized nanoparticles (crossectional view with zooming, X = 10 K) while Fig. 3(b) shows the zoomed micrograph (crossectional view with zooming, X = 20 K). The SEM image shows that the particles are spherical and are homogeneously distributed. Also, the particles appeared in a uniform and consistent shape.

3.4. UV-vis characterization

The optical property of the synthesized *p*-CdS nanoparticles is examined by UV-vis. spectroscopy at room-temperature and is shown in Fig. 4(a). The observed spectrum showed a single absorption peak at 480 nm. It is observed that absorption of synthesized material is sharp.

Table 1
Elemental composition observed by EDS.

Sample	Cu	Cd	S
Cu-doped CdS nanoparticles (%)	13.73	40.71	45.56

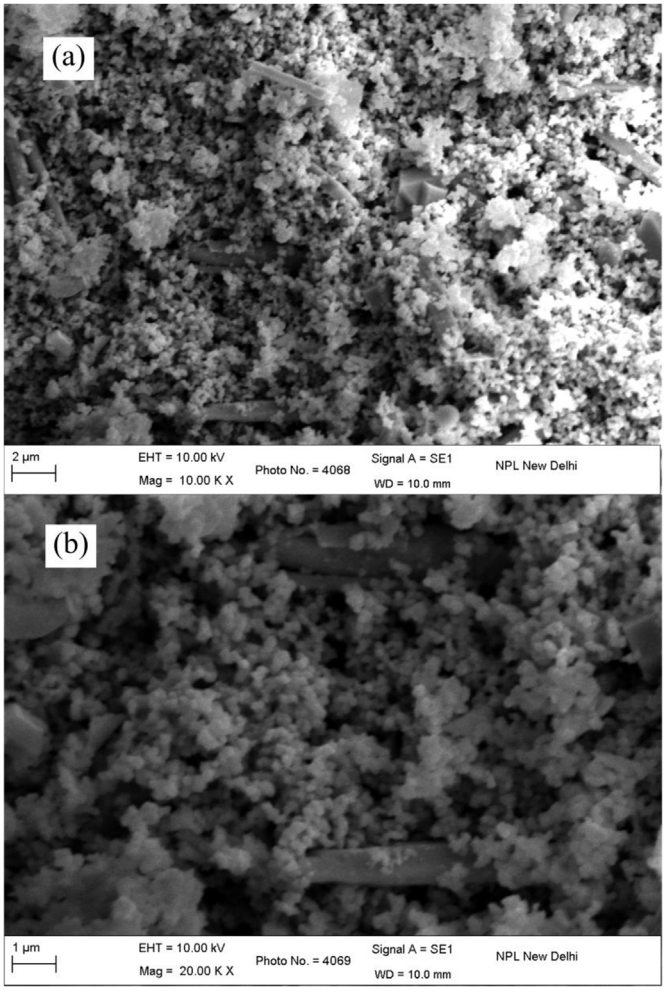

Fig. 3. (A) SEM of *p*-CdS nanoparticles with X = 10 K. (b) SEM of Cu-doped CdS nanoparticles with X = 20 K.

This may reveal that the Cu-doped CdS nanoparticles is a direct bandgap that shows absorption due to the electronic transitions from the valence band to the conduction band. The energy band gap (Eg) is determined from the optical absorption spectra using Tauc relation [14],

$$\alpha h\nu = A(h\nu - E_g)^n \tag{2}$$

where $\alpha$is the absorption coefficient, $h\nu$ is the photon energy, E_g is the band gap and n is a constant that determines the type of optical transitions (n = 1/2 and 3/2 for direct allowed and forbidden transition, respectively, and n = 2 and 3 for indirect allowed and forbidden transition, respectively). The bandgap is determined by extrapolating the straight line to zero absorbance, i.e., $(\alpha h\nu)^{\frac{1}{2}} = 0$and the plot is shown in Fig. 4(b). Thus, the band gap energy of the synthesized Cu-doped CdS nanoparticles is 2.03 eV. This value is shifted as compared to the bulk value and could be a consequence of a size quantization effect in the sample.

3.5. PL characterization

The PL spectra were employed to study the emission characteristics of synthesized nanoparticles. The room temperature PL spectrum of the Cu-doped CdS nanoparticles in the excitation wavelength range of 500–750 nm is shown in Fig. 4(c). The photoluminescence spectra of Cu doped CdS nanoparticles showed two peaks. The position of the first peak was found to be Stokes-shifted towards the higher wavelength value [15–17]. The shift in the peak may be due to an increase in the

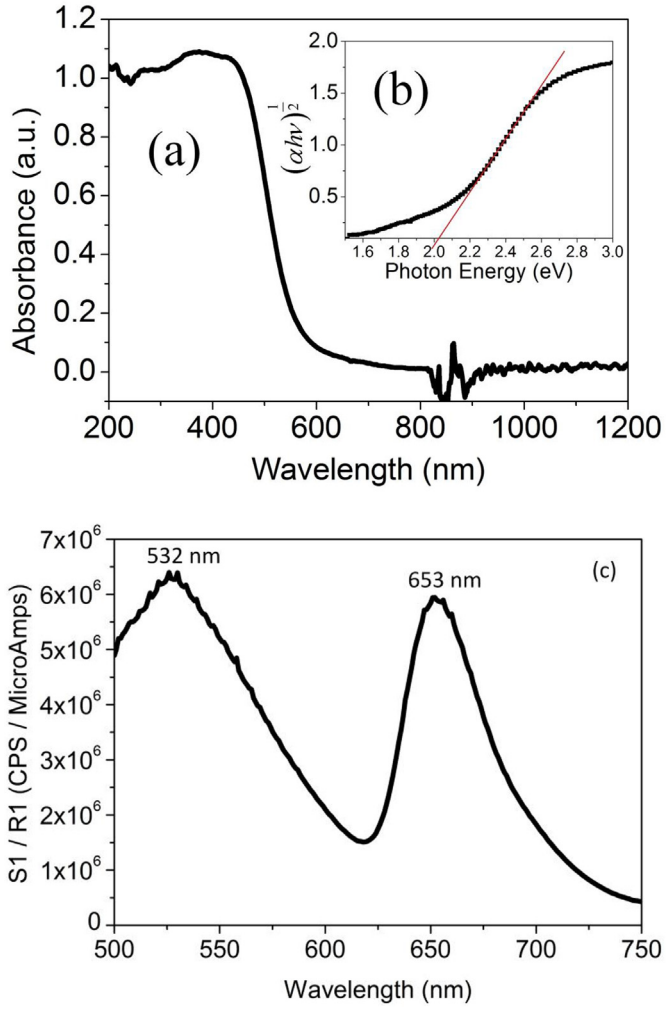

Fig. 4. (A) UV–vis absorption spectra, and (b)$(\alpha h\nu)^{\frac{1}{2}}$ vs $h\nu$, and (c) Photoluminescence spectrum of Cu-doped CdS nanoparticles at room temperature.

particle size. The green emission band centred at around 532 nm is the characteristic luminescence property of CdS due to the transition of electrons from shallow traps near the conduction band to sulphur vacancies present near the valence band [8] [18–20]. The other prominent peak of PL emission spectra of Cu doped CdS sample shows that Cu related orange-red emission is centred with maxima at 653 nm. The position of the second peak at 653 nm originates from a transition between the excited state and the ground state of the Cu^{+} ion within a nanocrystalline CdS lattice. The two peaks in the PL spectra confirmed the incorporation of Cu in the CdS matrix. The peaks are broad, indicating the formation of desired nanoparticles. As per the literature, the green emission band is associated to an electronic transition from the conduction band to an acceptor level due to interstitial sulphur and donor levels due to native defects in the Cu doped CdS lattice whereas the large emission band at 653 nm is attributed to a transition from either interstitial cadmium or copper vacancy to valence band [21].

3.6. Electrical characterization

I-V characteristics of the proposed device are shown in Fig. 5. The voltage is applied from −1 V to +1 V and the graph is plotted for current densities measured for dark current (I_d) and photo currents (I_{ph}) at an input power $(P_{in})_{50}$ at 50 mW/cm^2 and $(P_{in})_{100}$ at 100 mW/cm^2, respectively.

The source of illuminated light is white light from the solar simulator. The obtained I_d is negligible as compared to different I_{ph}.

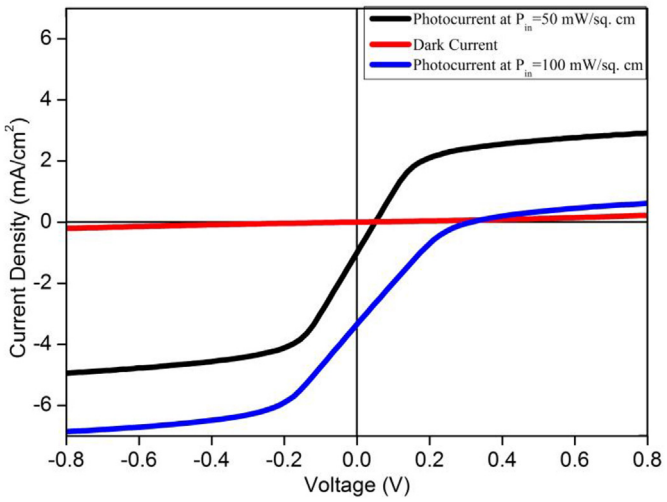

Fig. 5. *I-V* characteristics of fabricated glass/ITO/n-ZnO/p-CdS/Al photo-diode measured under dark and at light intensities at $(P_{in})_{50}$ and $(P_{in})_{100}$.

However, under forward bias condition, I_{ph} for $(P_{in})_{50}$ comes into saturation very quickly for a very small forward voltage (0.2 V) than for $(P_{in})_{100}$ at 0.4 V. Under forward bias operation of *p*-CdS/*n*-ZnO photodiode, as the intensity of illuminated light source increases, the depletion region becomes very small, and hence the photocurrent is contributed by the diffusion of excess photo-generated carriers in the neutral region of the photodiode.

Under reverse bias condition, the graph shows a similar trend as expected for a photodiode. An increase in the depletion region with the reverse bias voltage results in a significant photocurrent due to the drifting of the photo-generated excess carriers in the depletion region owing to the presence of a strong electric field in that region. Characterizations were conducted on the devices over several times, showing the same features.

Fig. 6(a) shows the graph plotted between gain and the applied voltage. The gain of the fabricated device is taken as the ratio of I_{ph} to the I_d. The graph shows an increase in gain with increase of the illumination. This may be due to Zener tunnelling that usually occurs in highly doped semiconductors under small bias voltage [22]. Further, the external quantum efficiency (EQE) is measured by the formula,

$$\mathrm{EQE} = \frac{hc}{q}\left(\frac{J_{SC}}{P_{in}}\right)A = 1240\left(\frac{J_{SC}}{P_{in}}\right)A \tag{3}$$

where h is Plank's constant, c is the velocity of light in free space, q is the elementary charge, J_{SC} is the short circuit current and A is the pixel area of the fabricated device. The EQE is found to be 95.42% for $(P_{in})_{100}$ and 30.69% for $(P_{in})_{50}$. Fig. 6(b) shows the maximum responsivity of the photodiode as a function of the applied bias. The value of the responsivity (R) is computed using the following relation [23].

$$R = \frac{I_{ph}}{P_{in}} \tag{4}$$

From Fig. 6(b), it is confirmed that the maximum responsivity is 1.6 A/W for $(P_{in})_{100}$ and 1.02 A/W for $(P_{in})_{50}$ intensities. The responsivity increases gradually for small reverse bias voltage, but it increases abruptly as the bias voltage tends towards −1 V. This phenomenon consolidates that an increase in responsivity with applied reverse bias voltage is due to the increase in the drift velocity of the photo-generated carrier with the increased electric field in the depletion region.

4. Conclusion

In summary, *p*-type Cu-doped CdS nanoparticles were synthesized via sol gel method. By using the as-syntheiszed nanoparticles, a thin

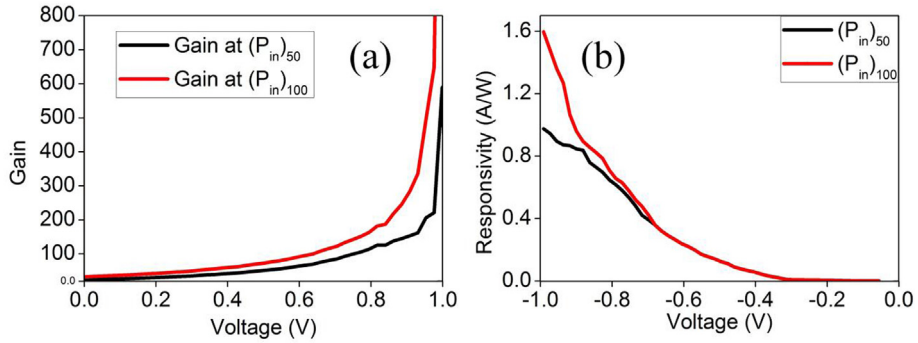

Fig. 6. (A) Gain of the photodiode, and (b) photo-response under reverse bias, measured at light intensities at $(P_{in})_{50}$ and $(P_{in})_{100}$.

film based glass/ITO/n-ZnO/p-CdS/Al heterojunction device have been proposed and demonstrated experimentally as a photodiode. A proposed device showed significantly improved results particularly for small bias voltage (−1 V to +1 V) with EQE (95.42%), gain (800) and reponsivity (1.6 A/W) as compared to other reported results for photodiodes. Thus, the proposed thin films grown on ITO substrate showed that the device under study can be explored as a potential photo-detector for photonic applications. The results revealed that the synthesized Cu-doped CdS nanoparticles are useful *p*-type material and an efficient replacement to high cost and low sensitive *p*-type material for opto-device fabrications.

Conflicts of interest

The authors declare that there is no conflict of interest.

Acknowledgment

This work is supported by SERB-DST (File No. EEQ/2016/000119).

References

[1] W.W. Xiong, J. Miao, P.Z. Li, Y. Zhao, B. Liu, Q. Zhang, [enH][Cu2AgSnS4]: a quaternary layered sulfide based on Cu–Ag–Sn–S composition, CrystEngComm 16 (2017) 5989–5992.
[2] D.H. Kim, J. Xiao, J. Song, Y. Huang, J.A. Roge, Stretchable, curvilinear electronics based on inorganic materials, Adv. Mater. 22 (2010) 2108–2124.
[3] W.W. Xiong, J. Miao, K. Ye, Y. Wang, B. Liu, Q. Zhang, Threading chalcogenide layers with polymer chains, Angew. Chem. Int. Ed. 54 (2015) 546–550.
[4] S. Suresh, Studies on the dielectric properties of CdS nanoparticles, Appl. Nanosci. 4 (2014) 325–329.
[5] Y. Deng, J. Yang, R. Yang, K. Shen, D. Wang, D. Wang, Cu-doped CdS and its application in CdTe thin film solar cell, AIP Adv. 6 (2016) 015203–1-015203-10.
[6] T. Lavanya, N.V. Jaya, Synthesis and characterization of pure CdS nanoparticles for optoelectronic applications, Trans. Indian Ceram. Soc. 70 (2011) 119–123.
[7] M.A.G. Pinilla, L.C. Moreno, G.G. Guzman, Optical and morphological properties of CdS nanoparticles thin films deposited by CBD process, Chalcogenide Lett. 8 (2011) 601–609.
[8] S. Qin, Y. Liu, Y. Zhou, T. Chai, J. Guo, Synthesis and photochemical performance of CdS nanoparticles photocatalysts for photodegradation of organic dye, J. Mater. Sci. Mater. Electron. 28 (2017) 7609–7614.
[9] L.L. Ma, H.Z. Sun, Y.G. Zhang, Y.L. Lin, J.L. Li, E. Wang, Y. Yu, M. Tan, J.B. Wang, Preparation, characterization and photocatalytic properties of CdS nanoparticles dotted on the surface of carbon nanotubes, Nanotechnology 19 (2008) 115709–1-115709-8.
[10] S.P. Mondal, S.K. Ray, Cadmium sulfide nanostructures for photovoltaic devices, Proc. Natl. Acad. Sci. Sect. A Phys. Sci. 82 (2012) 21–29.
[11] S.B. Rana, R.P.P. Singh, S. Arya, Structural, optical, magnetic and antibacterial study of pure and cobalt doped ZnO nanoparticles, J. Mater. Sci. Mater. Electron. 28 (2017) 2660–2672.
[12] S. Arya, P.K. Lehana, S.B. Rana, Synthesis of zinc oxide nanoparticles and their morphological, optical, and electrical characterizations, J. Electron. Mater. 46 (2017) 4604–4611.
[13] Z.R. Khan, M. Zulfequar, M.S. Khan, Chemical synthesis of CdS nanoparticles and their optical and dielectric studies, J. Mater. Sci. 46 (2011) 5412–5416.
[14] N.B.H. Mohamed, M. Haouari, N. Jaballah, A. Bchetnia, K. Hriz, M. Majdoub, H.B. Ouada, Optical and IR study of CdS nanoparticles dispersed in a new confined p-phenylenevinylene, Phys. B Condens. Matter 407 (2012) 3849–3855.
[15] V.P. Luna, S.O. Ruiz, E. Perez, M. Quintana, Single-walled carbon nanotubes as one-dimensional template for CdS nanoparticles growth, Phys. Status Solidi B 254 (2017) 1700197–1700201-1700197-5.
[16] B.S. Zou, R.B. Little, J.P. Wang, M.A. El-Sayed, Effect of different capping environments on the optical properties of CdS nanoparticles in reverse micelles, Int. J. Quant. Chem. 72 (1999) 439–450.
[17] N. Neelakandeswari, G. Sangami, N. Dharmaraj, N.K. Taek, H.Y. Kim, Spectroscopic investigations on the photodegradation of toluidine blue dye using cadmium sulphide nanoparticles prepared by a novel method, Spectrochim. Acta 78 (2011) 1592–1598.
[18] N.M. Vuong, N.D. Chinh, B.T. Huy, Y. Lee, CuO-decorated ZnO hierarchical nanostructures as efficient and established sensing materials for H_2S gas sensors, Sci. Rep. 6 (2016) 26736.
[19] S. Bellei, A. Nevin, A. Cesaratto, V. Capogrosso, H. Vezin, C. Tokarski, G. Valentini, D. Comelli, Multianalytical study of historical luminescent lithopone for the detection of impurities and trace metal ions, Anal. Chem. 87 (2015) 6049–6056.
[20] A. Fuhr, H.J. Yun, N.S. Makarov, H. Li, H. McDaniel, V.I. Klimov, Light-emission mechanism in $CuInS_2$ quantum dots evaluated by spectral electrochemistry, ACS Photonics 4 (2017) 2425–2435.
[21] N. Soltani, E. Saion, M.Z. Hussein, M. Erfani, A. Abedini, G. Bahmanrokh, M. Navasery, P Vaziri, Visible light-induced degradation of methylene blue in the presence of photocatalytic ZnS and CdS nanoparticles, Int. J. Mol. Sci. 13 (2012) 12242–12258.
[22] V. Qaradaghi, I. Mejia, M.Q. Lopez, Fabrication and analysis of thin film CdTe/CdS-based avalanche photodiodes, IEEE Electron. Device Lett. 38 (2017) 489–492.
[23] A.B. Yadav, A. Pandey, D. Somvanshi, S. Jit, Sol-gel-based highly sensitive Pd/n-ZnO thin film/n-Si Schottky ultraviolet photodiodes, IEEE Trans. Electron. Dev. 62 (2015) 1879–1884.